

## ORIGINAL RESEARCH ARTICLE

# Thermal modeling of a parabolic trough solar collector using finite element method

Armando Jesus Cetina Quiñones<sup>1</sup>, Ali Bassam<sup>2\*</sup>, Gandhi Samuel Hernandez Chan<sup>3</sup>, Jose Agustin Hernandez Benitez<sup>3</sup>, Ignacio Hernández Reyes<sup>4</sup>, David Lugo Chávez<sup>4</sup>

<sup>1</sup> Estudiante de Licenciatura de Ingeniería en Energías Renovables, Facultad de Ingeniería-UADY, Av. Industrias No Contaminantes por Anillo Periférico Norte s/n Apdo. Postal 150 Cordemex, Mérida, Yucatán, México.

<sup>2</sup> Facultad de Ingeniería-UADY, Av. Industrias No Contaminantes por Anillo Periférico Norte s/n Apdo. Postal 150 Cordemex, Mérida, Yucatán, México. E-mail: baali@correo.uady.mx

<sup>3</sup> Instituto Tecnológico de Mérida, Av. Tecnológico Km 4.5 S/N C.P 97118, Mérida, Yucatán México.

<sup>4</sup> División de Ingeniería Electromecánica del Instituto Tecnológico Superior de Centla, Calle Ejido S/n., Col. Siglo XXI, Frontera, Centla, Tabasco, C.P. 86750, México.

## ABSTRACT

The purpose of this work is to present the model of a Parabolic Trough Solar Collector (PTC) using the Finite Element Method to predict the thermal behavior of the working fluid along the collector receiver tube. The thermal efficiency is estimated based on the governing equations involved in the heat transfer processes. To validate the model results, a thermal simulation of the fluid was performed using Solidworks software. The maximum error obtained from the comparison of the modeling with the simulation was 7.6% at a flow rate of 1 l/min. According to the results obtained from the statistical errors, the method can effectively predict the fluid temperature at high flow rates. The developed model can be useful as a design tool, in the optimization of the time spent in the simulations generated by the software and in the minimization of the manufacturing costs related to Parabolic Trough Solar Collectors.

**Keywords:** Solar Energy; Numerical Simulation; Photothermal Systems; Thermal Efficiency; Thermal Efficiency

## ARTICLE INFO

Received: 2 October 2022  
Accepted: 4 November 2022  
Available online: 16 November 2022

## COPYRIGHT

Copyright © 2022 Armando Jesus Cetina Quiñones, et al.  
EnPress Publisher LLC. This work is licensed under the Creative Commons Attribution-NonCommercial 4.0 International License (CC BY-NC 4.0).  
<https://creativecommons.org/licenses/by-nc/4.0/>

## 1. Introduction

Environmental pollution by greenhouse gases is a problem that has arisen over the last few decades. These gases are produced by different factors, including the combustion of fossil fuels, water vapor, the use of fertilizers in agricultural fields, and the venting of natural gas, among others. The considerable increase in these gases, such as carbon dioxide (CO<sub>2</sub>), sulfur dioxide (SO<sub>2</sub>) and nitrous oxide (NO<sub>x</sub>), leads to devastating consequences that have a direct impact on climate change<sup>[1]</sup>. For this reason, there is a current global trend focused on the use of alternative energy sources as a measure to mitigate emissions of these harmful gases and other pollutants into the atmosphere<sup>[2]</sup>.

Solar energy is one of the renewable energy sources that attract more attention due to its abundance, cleanliness and the fact that it does not generate any pollution<sup>[3]</sup>. Within this energy source is the technology of solar concentrators which is one of the most developed currently and employed for electric power generation<sup>[4]</sup>. Concentrator-type solar collectors are capable of producing high temperatures (over 400 °C). This makes them a feasible and promising technology for solar desali-

nation, solar chemistry applications, solar cooling (absorption and adsorption), solar hydrogen production and Concentrated Solar Power Plants (CSP)<sup>[5]</sup>.

A CCP captures radiant energy from the sun and concentrates it in a receiver tube located on the focal axis of the parabola through which a working fluid is circulated, transforming solar radiation into useful thermal energy. The heat transfer analysis of these collectors is important for the calculation of thermal losses and the sizing of the solar power plant during preliminary design<sup>[6]</sup>.

Given the importance of heat transfer analysis in the CCP, different models have been developed over the last few years. Nwosu<sup>[7]</sup> developed a thermal model using the finite element method to a receiver tube with evacuated glass cover, in which he obtained the best gain at high heat fluxes. On the other hand, Liang<sup>[8]</sup> compared different heat transfer models in CCP by which he concluded the unnecessary of contemplating heat conduction in receiver tubes with evacuated cover. More recent studies such as Uzgoren<sup>[9]</sup>, in which he evaluated a CCP in transient state by means of a mathematical model developed by the finite volume method, validating it with experimental data, obtaining non-significant errors. Finally, Jaramillo<sup>[10]</sup> performed an analysis of the thermal efficiency of a CCP by inserting twisted tapes inside the receiver tube, obtaining a 3.5% increase in thermal efficiency under controlled conditions.

The characterization of a CCP is of utmost importance, since it allows to know the different phenomena that occur in it. One of these is the behavior of the temperature along the receiver tube, from the inlet to the outlet. This allows to observe the phenomenon of heat transfer from the receiver tube to the fluid, as well as to predict the phase change of the fluid, guaranteeing the obtaining of steam for the generation of electricity. In the same way, modeling allows characterizing a CCP under different conditions without the need to resort to experimentation and to have a general concept of the thermal behavior of the fluid.

The objective of this work is to model a CCP by means of the first law of thermodynamics using the Finite Element Method (FEM). This

method allows obtaining a fluid temperature profile by discretizing the receiver tube in a finite number of elements called nodes. Likewise, the validation of the model is presented by means of a simulation of the flow temperature implemented in the Solidworks® software.

## 2. Methodology

A CCP is a solar concentrating system consisting of a reflecting sheet that captures the sun's rays and concentrates them on a receiver tube located on the focal axis of the parabola. **Figure 1** shows the design and basic components of a CCP.

Two of the important parameters that characterize a CCP are the temperature at the outlet of the receiver tube and the thermal efficiency. The former describes the heat gained by the working fluid, which allows the development of prototypes that can be optimized for processes requiring specific temperatures. Thermal efficiency, on the other hand, allows obtaining the ratio of useful energy with respect to the energy input to the system.

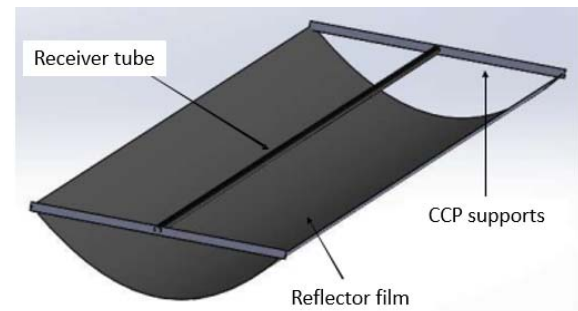


**Figure 1.** Basic components of a CCP.

### 2.1 Thermal analysis of the CCP

In a solar concentrating system, one of the important parameters is the optical efficiency, which is calculated by Equation 1.

$$\eta_o = \rho\tau\alpha\gamma(1 - A_f \tan(\theta))\cos(\theta) \quad (1)$$

Where,  $\rho$  is the reflectivity of the reflective sheet,  $\tau$  is the transmissivity of the tube envelope,  $\alpha$  is the absorptivity of the receiver tube,  $\gamma$  is the interception factor,  $A_f$  is the geometrical factor of the collector and  $\theta$  is the angle of incidence of the solar rays<sup>[11]</sup>. For the thermal analysis of the CCP, single-phase flow is considered, being water the working fluid. Likewise,

conduction losses are considered negligible since the supports of the receiving pipe are assumed to be insulated. **Figure 2** shows the model of the receiver pipe and the representation of the thermal losses as a network of resistances.

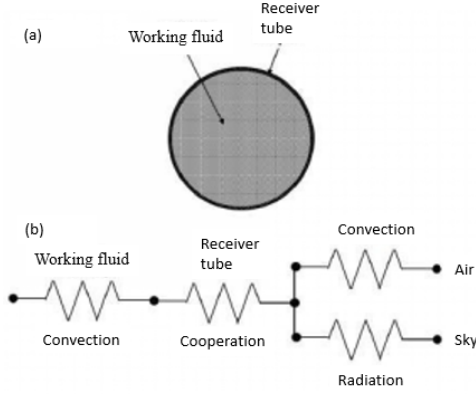


**Figure 2.** Fi Model of the receiver tube: (a) nomenclature; (b) thermal resistance network for cross section.

$$Nu_v = 0.3 + \frac{0.62 \Re_v^{1/2} Pr_v^{1/3}}{[1 + (0.4/Pr_v)^{2/3}]^{1/4}} \left[ 1 + \left( \frac{\Re_v}{282000} \right)^{5/8} \right]^{4/5} \quad (4)$$

Where,  $Pr_v$  is the Prandtl number for air and  $\Re_v$  is the Reynolds number of air, which is calculated by Equation 5:

$$\Re_v = \frac{VD_e}{\nu} \quad (5)$$

Where,  $V$  is the wind speed and  $\nu$  is the kinematic viscosity of the air.

On the other hand,  $h_r$  is estimated by Equation 6:

$$h_r = 4\sigma\varepsilon_r T_r^3 \quad (6)$$

Where,  $\sigma$  is the Stefan-Boltzmann constant,  $\varepsilon_r$  is the emissivity and  $T_r$  the receiver tube temperature, calculated as:

$$Nu_w = \begin{cases} (1 - \xi)Nu_{lam,2300} + \xi Nu_{turb,4000} \\ \left( \frac{f_f}{8} \right) (\Re_w - 1000) \left( 1 + d^{\frac{2}{3}} \right) Pr_w \left( \frac{Pr_w}{Pr_v} \right)^{0.11} \\ 1 + 12.7 \sqrt{\left( \frac{f_f}{8} \right) (Pr_w^{\frac{2}{3}} - 1)} \end{cases} \quad \begin{cases} \Re_w < 2300 \\ 2300 < \Re_w < 4000 \\ \Re_w > 4000 \end{cases} \quad (9)$$

To estimate the convective and radiative heat transfer losses in the receiver, the overall coefficient of thermal losses must be found  $U_L$  calculated as:

$$U_L = h_v + h_r \quad (2)$$

Where,  $k_v$  is the thermal conductivity of air,  $D_e$  the where the coefficient,  $h_v$  represents the convective heat transfer loss, and  $h_r$  the radiative heat loss,  $h_v$  is calculated by Equation 3:

$$h_v = \frac{k_v}{D_e} Nu_v \quad (3)$$

External diameter of the receiving pipe  $y Nu_v$  the Nusselt number which can be estimated by the Churchill and Bernstein equation as<sup>[12]</sup>:

$$T_r = T_{e,m} + \frac{\eta_o G_b C_o}{h_w} \quad (7)$$

Being  $T_{e,m}$  the maximum fluid temperature at the outlet,  $G_b$  the direct solar radiation,  $C_o$  the concentration factor and  $h_w$  the convective heat transfer coefficient inside the receiver tube, which is found as:

$$h_w = \frac{k_w}{D_i} Nu_w \quad (8)$$

Hence,  $k_w$  is the thermal conductivity of water,  $D_i$  is the internal diameter of the pipe and  $Nu_w$  the Nusselt number of water which depends on the type of flow, and is calculated as<sup>[13]</sup>:

From Equation 9,  $Pr_w$  is the Prandtl number of the water,  $d$  is a factor calculated as the ratio of the internal diameter of the pipe to its total length,  $D_i$  is the internal diameter of the receiving pipe  $y\xi$  is a factor which is calculated by Equation 10.

$$\xi = \frac{\Re_w - 2300}{4000 - 2300} \quad (10)$$

Similarly,  $f_f$  is the friction factor and is estimated by the Chen equation<sup>[14]</sup>:

$$f_f = \frac{1}{\left\{ -2 \log \left( \frac{1}{3.7065} \left( \frac{r_r}{D_i} \right) - \frac{5.0452}{\Re_w} \log \left[ \frac{1}{2.8257} \left( \frac{r_r}{D_i} \right)^{1.1098} + \frac{5.8506}{\Re_w^{0.8981}} \right] \right\}^2} \quad (11)$$

Where,  $r_r$  is the roughness of the material, of which the pipe is made. On the other hand,  $Nu_{lam} = 4.36$ ,  $Nu_{turb,4000}$  is calculated by the turbulent flow equation  $\Re > 4000$ , taking  $\Re_w = 4000$ ,  $Pr_w = 0.7$ ,  $d = 0.0001$  and  $\frac{Pr_w}{Pr_p} = 1$ . The Reynolds number of water ( $\Re_w$ ) is calculated as:

$$\Re_w = \frac{4\dot{m}}{\pi D_i \mu_w} \quad (12)$$

Where,  $m$  is the mass flow, and  $\mu_w$  is the dynamic viscosity of the water.

Subsequently, the removal factor is calculated  $F_R$  as<sup>[15]</sup>:

$$F_R = \frac{\dot{m}c_p}{A_r U_L} \left[ 1 - \exp \left( \frac{-U_L F' A_r}{\dot{m}c_p} \right) \right] \quad (13)$$

Where,  $A_r$  is the area of the receiver pipe,  $c_p$  is the specific heat of water, and  $F'$  is the collector efficiency factor calculated as:

$$F' = \frac{1}{\frac{1}{U_L} + \frac{D_e}{h_w D_i} + \left[ \frac{D_e}{2k_c} \ln \left( \frac{D_e}{D_i} \right) \right]} \quad (14)$$

Of which  $k_c$  is the thermal conductivity of the receiver pipe.

The equation relating the energy gain of a CCP is:

$$\dot{m}c_p (T_e - T_i) = F_R (\eta_o A_a G_b - A_r U_L (T_i - T_a)) \quad (15)$$

Where,  $T_i$  is the initial temperature of the fluid, and  $A_a$  is the aperture area of the reflecting sheet. Therefore, the fluid outlet temperature is given as:

$$T_e = T_i + \frac{F_R [\eta_o A_a G_b - A_r U_L (T_i - T_a)]}{\dot{m}c_p} \quad (16)$$

Where,  $T_a$  is the ambient temperature. Finally, by the first law of thermodynamics, the thermal efficiency of the CCP is as:

$$\eta_t = F_R \left[ \eta_o - \frac{U_L}{C_o} \left( \frac{T_i - T_a}{G_b} \right) \right] \quad (17)$$

## 2.2 The finite element method

The finite element method (FEM) is a numerical method for the solution of engineering problems commonly employed in those involving a high degree of mathematical complexity, as well as physical-mathematical, with applications in problems of heat transfer, fluid flow, mass transport, etc.<sup>[16]</sup>.

The FEM involves several numerical methods that are used to obtain results approximating the real value. In this work, the Galerkin method was employed, which is a method with an error of about 7% of the true value, and with a high degree of accuracy<sup>[17]</sup>. The Galerkin method is stated as:

$$\int_{x_i}^{x_j} N_{i,j}(x) R(x; T) dV = 0 \quad (18)$$

Where:

$x_i$  is the first node of the system.

$x_j$  is the nodal length of the system.

$N_{i,j}$  is the nodal test function,  $N_i = 1 - \frac{x}{L_n}$ ,

$N_j = 1 - \frac{x}{L_n}$ , of which,  $L_n$  is the nodal length.

$R(x; T)$  is the residual function, which measures the difference between the test solution and the real solution, this being Equation 15;  $dV$ : is the volume differential.

From Equation 15,  $T_e - T_i$  is rewritten as differential.

Thus, applying Galerkin's method to this equa-

$$\frac{dT(x)}{dx} N_{i,j}(x) dV = F_R [\eta_o G_b W_a - U_L \pi D_e (T_i - T_a)] \int_0^{L_n} N_{i,j}(x) dV - \dot{m} c_p \int_0^{L_n} \quad (19)$$

Where,  $W_a$  is the opening length of the sheet. Considering that  $N_{i,j}$  decomposes to  $N_i$  and  $N_j$  and that the temperature at node  $i$  multiplied by its respective nodal length, plus the temperature at

tion leaves:

node  $j$  multiplied by its nodal length up to that point is expressed as  $T(x) = N_i(x)T_i + N_j(x)T_j$ , Equation 19 is rewritten in matrix form as:

$$\dot{m} c_p \int_0^{L_n} \begin{bmatrix} N_i(x) \frac{dN_i(x)}{dx} & N_i \frac{dN_j(x)}{dx} \\ N_j(x) \frac{dN_i(x)}{dx} & N_j \frac{dN_j(x)}{dx} \end{bmatrix} \begin{Bmatrix} T_i \\ T_j \end{Bmatrix} dx = F_R [\eta_o G_b W_a - U_L \pi D_e (T_i - T_a)] \int_0^{L_n} \begin{bmatrix} N_i(x) \\ N_j(x) \end{bmatrix} dx \quad (20)$$

Analytically integrating and simplifying the terms of

Equation 20, it is finally left as:

$$\frac{\dot{m} c_p}{2} \begin{bmatrix} -1 & 1 \\ -1 & 1 \end{bmatrix} \begin{Bmatrix} T_i \\ T_j \end{Bmatrix} = \frac{F_R [\eta_o G_b W_a - U_L \pi D_e (T_i - T_a)] L_n}{2} \begin{bmatrix} 1 \\ 1 \end{bmatrix} \quad (21)$$

Equation 21 represents the fluid temperature along the receiving pipe simplified for 2 nodes. To obtain a temperature profile it is necessary to work with a larger number of nodes.

### 2.3 Computational development

The FEM was developed in the MATLAB programming environment. The flowchart implemented for the programming are presented in **Figure 3**. First, the length of the receiver tube ( $L_i$ ) and then the number of nodes ( $N_n$ ) were initialized in order to calculate the nodal distance ( $L_n$ ). Subsequently, the generated matrix and the generated vector are assembled. The boundary conditions for both are included and the temperature profile is calculated by solving the assembled matrix.

For the validation of the CCP model, Solidworks software was used to estimate the temperature behavior of the working fluid along the receiving pipe using its flow simulation tool, which allowed observing the phenomena presented in the pipe. For the validation, four phases were followed as shown in **Figure 4**.

Phase 1: The CCP is designed in the software as shown in **Figure 4**.

Phase 2: The input parameters with which the simulation will be performed are included. These parameters are explained in the results section.

Phase 3: The simulation is carried out considering the parameters included in Phase 2, as well as the boundary conditions involved in the thermal behavior of the fluid temperature.

Phase 4: In this last phase, the results obtained from the software simulation are compared with those obtained from the FEM modeling, thus validating the developed model.

## 3. Results and discussion

This section presents the results obtained from the modeling developed using the FEM. A thermal analysis of the effects of seven parameters included in the modeling performing in order to observe the behavior of the fluid along the receiver tube, as well as the behavior of the thermal efficiency of the CCP. Finally, the results and the errors obtained statistically from the model developed through the FEM are compared with the simulation carried out using the Solidworks software through its flow simulation tool.

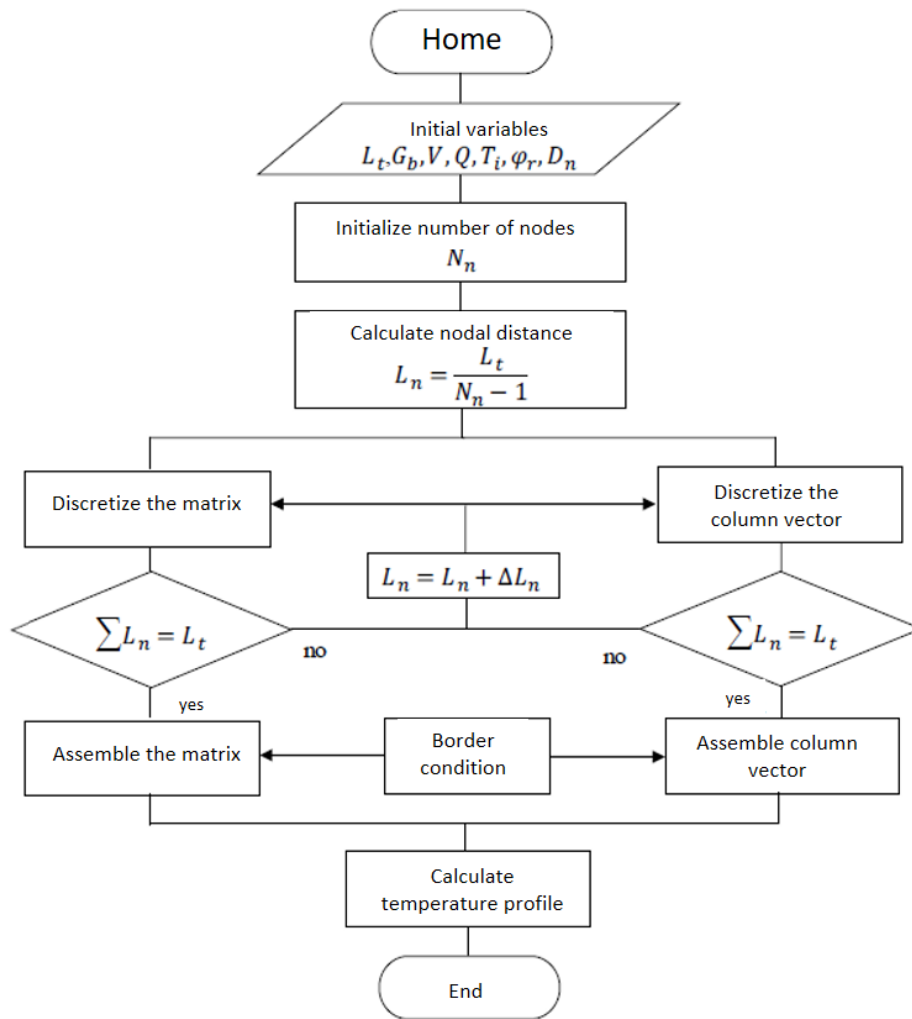


Figure 3. FEM flowchart.



Figure 4. Phases implemented for the validation of the CCP thermal model.

### 3.1 Effects of input parameters on fluid temperature

For the modeling, seven nominal parameters were used, which were varied to observe the behavior of the water temperature along the receiving pipe and the thermal efficiency of the CCP. These parameters include the direct solar irradiance ( $G_b$ ) (varies from 500 to 1,000  $W/m^2$ ), the wind speed ( $V$ ) (from 1 to 6  $m/s$ ), the ambient temperature ( $T_a$ ) (from 25 to 35  $^{\circ}C$ ), the flow rate ( $Q$ ) (from 1 to 6  $l/min$ ), the initial fluid temperature ( $T_i$ ) (from 35 to 60  $^{\circ}C$ ), the edge angle of the CCP ( $\phi_r$ ) (from 30 to 90  $^{\circ}C$ ), and the nominal diameter of the receiver pipe ( $D_n$ ) (assigned the values of 1/2, 3/4, 1, 1  $\frac{1}{2}$

and 2 inches, respectively).

Figure 5 shows the different results obtained from the effects of the variation of each of the parameters mentioned above on the fluid temperature. Figure 5(a) presents the effect of irradiance, and a higher heat gain is observed at high irradiances because the heat flux to the receiver tube is higher under these conditions. Similarly, Figure 5(b) presents the variation of the wind speed, and a decrease of the fluid heat gain is observed when this parameter increases, because it is lower at high wind speeds due to the increase of external convective losses. Figure 5(c) presents the variation of the flow rate at the inlet of the receiver tube and shows



a lower thermal gain by the fluid when the flow rates are high due to higher convective losses inside the receiver tube. On the other hand, **Figure 5(d)** reflects the variation of the initial fluid temperature of the CCP receiver tube, from which a higher thermal gain gradient was obtained when this parameter increases, due to the fact of having a high useful heat at the inlet of the receiver tube. **Figure 5(e)** presents the variation of the edge angle, in which the highest thermal gain was obtained for the edge angle of 90°, due to the fact that the increase in the receiving area of the sheet produces a higher concentration factor, and thus a higher concentrated heat flux to the receiver tube. Finally, **Figure 5(f)**

represents the variation of the nominal diameter and its effect on the fluid temperature. The increase of this parameter leads to higher convective losses due to the larger area of the receiver tube. However, the concentration factor is higher when the nominal diameter decreases. For this reason, a nominal diameter must be found, which is optimal for minimizing convective losses and maximizing the thermal gain of the fluid. For this work, this diameter was 1 inch. As for the efficiency performance, seven cases were included, each of which was assigned a designated value for each nominal parameter, as shown in **Table 1**.

**Table 1.** Cases for modeling the thermal efficiency of the CCP

Case	Irradiance ( $G_b$ )	Wind speed (V)	Ambient Temperature ( $T_a$ )	Flow rate (Q)	Initial temperature ( $T_i$ )	Edge angle ( $\phi_r$ )	Nominal diameter ( $D_n$ )
I	500	1	25	1	35	30	½
II	600	2	27	2	40	40	¾
III	700	3	29	3	45	50	1
IV	800	4	31	4	50	60	1½
V	900	5	33	5	55	70	2
VI	1000	6	35	6	60	80	-
VII	-	-	-	-	-	90	-

**Figure 6** shows the thermal efficiency plots  $\eta_t$  for each case in **Table 1**. It is observed that parameters such as irradiance, flow rate, ambient temperature and edge angle are directly proportional to the thermal efficiency. These parameters influence in the same way as the fluid temperature along the receiver tube presented in **Figure 5**, i.e., the increase of any of these parameters involved generates higher thermal gain by the working fluid. On the other hand, wind speed and initial temperature are inversely proportional, which means that the increase of these parameters produces lower thermal gain of the flow. Likewise, it is observed that in the efficiency behavior for the variation of the nominal diameter, an optimum diameter of 1 inch was obtained. For diameters larger than this, the thermal efficiency decreases. Finally, the highest thermal efficiency was obtained in the variation of the ambient temperature, at 35 °C, reaching a value of 72%.

### 3.2 Validation of the thermal model

For the validation of the model, Solidworks software was used as a simulation tool. In this section, several simulations perform considering the

same input variables that were considered in the simulation developed with the FEM of the thermal model of the CCP, as an example of this simulation with the Solidworks software. **Figure 7(a)** shows the temperature at the outlet of the receiver pipe as a cross-sectional plot. In this graph it can be seen that the red section at the outlet corresponds to a temperature of approximately 42 °C, on the other hand, from **Figure 5(a)**, the approximate temperature corresponding to the irradiance of 900 W/m<sup>2</sup> for the non-evacuated tube is 41.6 °C considering the same parameters used in the thermal modeling with the FEM. This temperature agrees with the temperature obtained in Solidworks because this irradiance was one of the nominal parameters in the simulation, keeping the other parameters invariant, both in the modeling and in the simulation. The calculation times corresponding to the simulation with the Solidworks software were approximately 45 to 58 min. On the other hand, **Figure 7(b)** shows the cut-off graph of the receiver tube that represents the temperature behavior along it. The change of the fluid temperature is observed as it passes along the receiver tube, where the red color represents the highest temperature.

Finally, **Table 2** shows the values obtained from the modeling and simulation, with their respective errors, for which the flow rate was the parameter to be varied, since this is one of those that generate the greatest gradients in the fluid outlet temperature, as can be seen in **Figure 5(c)**.

Similarly, the maximum error obtained was 7.6 % for the minimum flow rate used, and the minimum error was 0.5% for the highest flow rate. Therefore, the results of the developed model are close to the Solidworks simulation and can effectively predict the fluid temperature behavior at high flow rates.

tively predict the fluid temperature behavior at high flow rates.

**Table 2.** Comparison of modeling and simulation results for each flow variation

Flow rate	MEF	Solidworks	Error
1 l/min	53.70 °C	49.61 °C	7.6 %
2 l/min	44.55 °C	42.41 °C	4.8 %
3 l/min	41.65 °C	41.33 °C	0.7 %
4 l/min	40.06 °C	39.74 °C	0.8 %
5 l/min	39.07 °C	38.82 °C	0.6 %
6 l/min	38.40 °C	38.20 °C	0.5 %

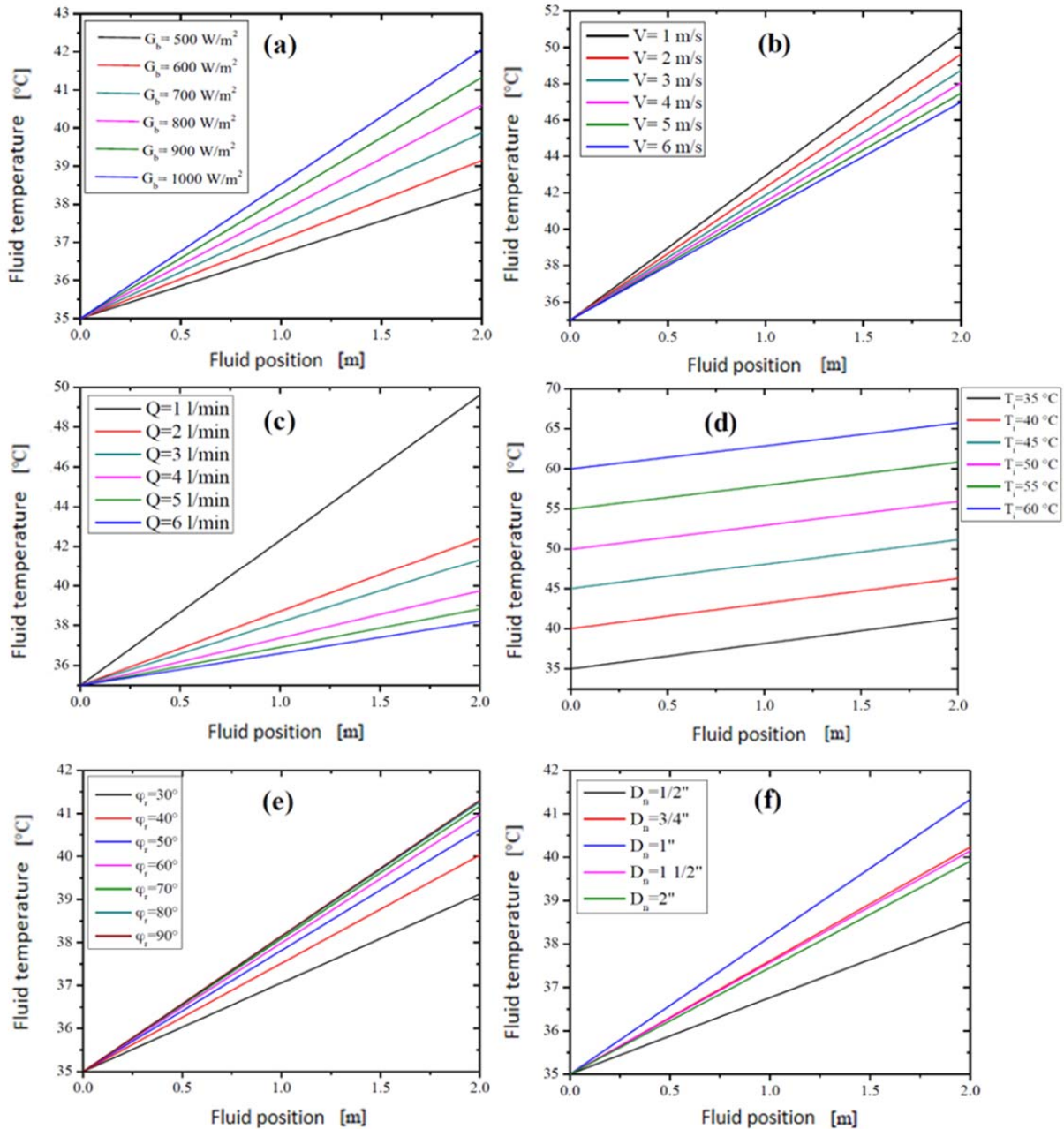


**Figure 5.** Effects of nominal parameters on fluid temperature: **5(a)** Effect of irradiance; **5(b)** effect of wind speed; **5(c)** effect of flow rate; **5(d)** effect of initial fluid temperature; **5(e)** effect of edge angle; **5(f)** effect of nominal diameter.



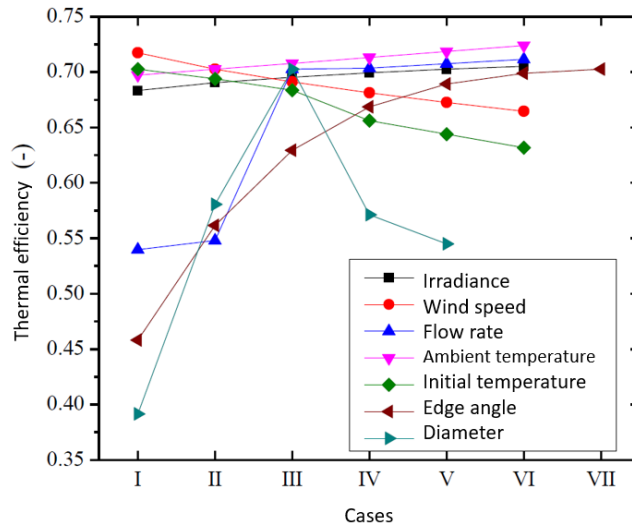


Figure 6. Thermal efficiency behavior for each case.

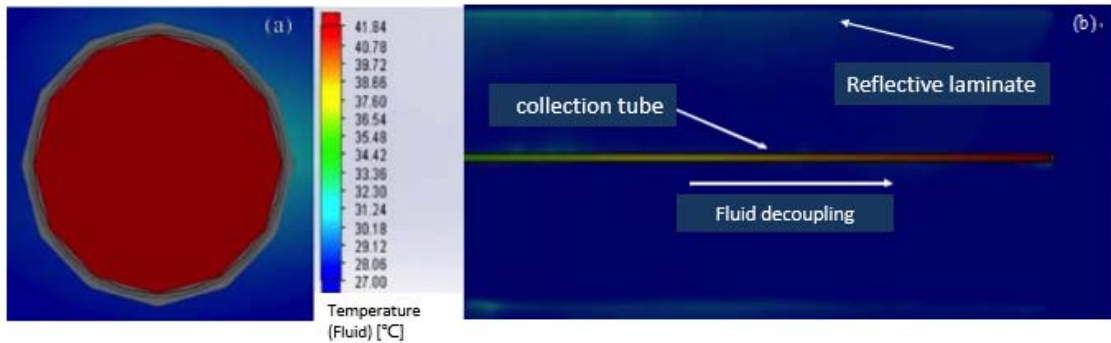


Figure 7. Graph of the thermal distribution of the fluid temperature: (a) outlet of the receiver tube; (b) along the receiving tube.

## 4. Conclusions

In the present work, a physical model for heat transfer in a Parabolic Trough Solar Concentrator (PCC) was developed. In the solution of the reported model equations, the Finite Element Method (FEM) was used as a modeling tool. The physical model developed is capable of calculating the temperature distribution of the working fluid along the CCP receiver tube. Likewise, the model allows the estimation of the CCP efficiency through a thermal analysis based on the first law of thermodynamics. The temperature distribution along the CCP receiver tube was obtained as a function of seven input parameters (solar irradiance, wind speed, ambient temperature, flow rate, initial fluid temperature, CCP edge angle and nominal diameter of the receiver tube), which were varied to study the behavior of the fluid temperature as a function of these parameters. The results obtained in the FEM modeling were validated by simulating the fluid using Solidworks software through its flow simulation

tool. The validation of the developed model reports a maximum error of 7.6% between the theoretical model and the Solidworks software. The model developed in this work is a useful tool to predict the temperature behavior of the working fluid under different environmental and operating conditions. The advantage of this model, in comparison with the Solidworks software, are the short calculation times, because, with the software, this time is approximately 45 to 58 minutes, while using MATLAB, this calculation does not exceed 30 seconds. As future work, it is desired to compare the results obtained from the thermal modeling with experimental results of the CCP, so that the developed model can be validated and can be used in the sizing and characterization of the CCP.

## Conflict of interest

The authors declared that they have no conflict of interest.

## References

1. Kalogirou SA. Solar thermal collectors and applications. *Progress in Energy and Combustion Science* 2004; 30(3): 231–295.
2. May Tzuc O, Bassam A, Escalante Soberanis MA, *et al.* Modeling and optimization of a solar parabolic trough concentrator system using inverse artificial neural network. *Journal of Renewable and Sustainable Energy* 2017; 9(1): 013701.
3. May O, Ricalde LJ, Ali B, *et al.* Neural network inverse modeling for optimization. In *Artificial Neural Networks-Models and Applications*. Intech; 2016.
4. Fernandez-Garcia A, Zarza E, Valenzuela L, *et al.* Parabolic-trough solar collectors and their applications. *Renewable and Sustainable Energy Reviews* 2010; 14(7): 1695–1721.
5. Tzivanidis C, Bellos E, Korres D, *et al.* Thermal and optical efficiency investigation of a parabolic trough collector. *Case Studies in Thermal Engineering* 2015; 6: 226–237.
6. Padilla RV, Demirkaya G, Goswami DY, *et al.* Heat transfer analysis of parabolic trough solar receiver. *Applied Energy* 2011; 88(12): 5097–5110.
7. Nwosu NP. Finite-element analysis of an absorber in an evacuated solar tube heat exchanger employing the Galerkin method. *International Journal of Sustainable Energy* 2009; 28(4): 247–255.
8. Liang H, You S, Zhang H. Comparison of different heat transfer models for parabolic trough solar collectors. *Applied Energy* 2015; 148: 105–114.
9. Uzgoren E. One-dimensional transient thermal model for parabolic trough collectors using closed-form solution of fluid flow. *International Exergy, Energy and Environment Symposium (IEEES-8)*; 2016.
10. Jaramillo OA, Borunda M, Velazquez-Lucho KM. *et al.* Parabolic trough solar collector for low enthalpy processes: An analysis of the efficiency enhancement by using twisted tape inserts. *Renewable Energy* 2016; 93: 125–141.
11. Duffie JA, Beckman WA. *Solar engineering of thermal processes*. 3<sup>rd</sup> ed. New York: Wiley; 2013.
12. Cengel YA, Ghajar A. *Heat and mass transfer*. New York: McGraw-Hill Publishers; 2011.
13. Gnielinski V. On heat transfer in tubes. *International Journal of Heat and Mass Transfer* 2013; 63: 134–140.
14. Fernández-García A, Rojas E, Pérez M, *et al.* A parabolic-trough collector for cleaner industrial process heat. *Journal of Cleaner Production* 2015; 89: 272–285.
15. Kalogirou SA. *Solar energy engineering: Processes and systems*. Academic Press; 2013.
16. Baskharone EA. *The finite element method with heat transfer and fluid mechanics applications*. Cambridge University Press; 2013.
17. Nithiarasu P, Lewis RW, Seetharamu KN. *Fundamentals of the finite element method for heat and mass transfer*. New York: John Wiley & Sons; 2016.